Journal of Sound and Vibration (2001) **242**(2), 321–331
doi:10.1006/jsvi.2000.3351, available online at http://www.idealibrary.com on IDEAL®

EXCITATION FORCE IDENTIFICATION OF AN ENGINE WITH VELOCITY DATA AT MOUNTING POINTS

J. S. TAO, G. R. LIU AND K. Y. LAM

Institute of High Performance Computing, 89-*C Science Park Drive* #02-11/12, *The Rutherford*, *Singapore* 118261, *Singapore. E-mail*: *taojinsheng@yahoo.com*

(*Received* 29 *May* 2000, *and in final form* 11 *October* 2000)

This paper describes how to reconstruct the excitation force of a typical engine from the measured velocity data at mounting points. The theoretical analysis is carried out at first to get the equations for the force re-construction. It indicates that with the full information of velocity (amplitude and phase) at all mounting points, the excitation force and moment at the center of gravity of engine can be exactly retrieved. Due to the difficulty in measuring the absolute values of the phases, further study is carried out to investigate the possibility to reconstruct the force and moment only with the velocity amplitude as well as the phase difference between three directions at each mounting point. A group of overdetermined equations are derived and solved with optimization methods rather than the conventional numerical method. It is found that with combination of genetic and gradient-based algorithms, the excitation force and moment of engine can be well-established based on the velocity spectra and phase angle difference of velocities.

1. INTRODUCTION

The excitation force of an engine is normally calculated based on the engine parameters [1, 2]. This method requires substantial data of engine that is sometimes difficult to be exactly measured, especially the rolling moment caused by a gas explosion. The coupling of engine to other equipment, e.g., fan or propeller, makes it even worse. However, the exact value of an engine excitation force is valuable for the optimal design of engine mounting system [2] or detecting any design or operational problems inside the engine. This is a typical inverse problem in vibration control which has recently received more attention [3].

The inverse problem to identify the excitation force is normally based on the measurement of frequency response transfer functions [4]. The response of a structure to an artificial excitation is measured at different locations on the structure so as to build the matrix of transfer function. This method is useful for a linear mechanical system subject to multi-point excitation. However, in the engine vibration control, the required value is the overall force and moment at the center of gravity (c.g.) of engine which cannot be directly identified by the transfer function method. On the other hand, the transfer function method is also too complicated for the force identification only at the c.g.

This paper presents a method to identify the engine excitation forces at c.g. from the measured velocities at mounting points. It should also be applicable to other rotating machines. To avoid foundation effects, the engine is considered mounting with isolators which are much softer than those of the foundations. The analysis indicates that the mounting forces and moments can be fully re-constructed as long as the velocity spectra and

0022-460X/01/170321 + 11 $35.00/0

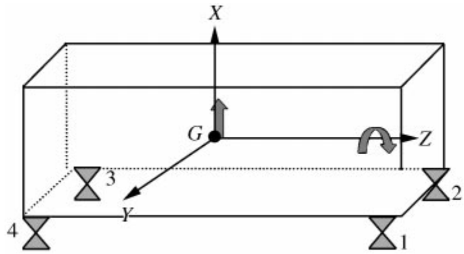

Figure 1. Engine mounting system.

the phase difference between three orthogonal directions (X, Y, Z) at each point are provided. The equations are derived and the combined genetic and gradient-based optimization methods are applied to solve these non-linear and overdetermined equations.

2. DIRECT EQUATIONS OF ENGINE MOTION

The engine is modelled as a rigid body that is supported by four vibration isolators fixed to a rigid floor as showed in Figure 1.

A rigid-body model is suitable for a structure whose geometry points remain fixed relative to one another [5]. The right-hand global co-ordinate system $Gxyz$ has its origin at the center of mass of the engine when in static equilibrium. The three orthogonal co-ordinate axes, which are shown in Figure 1, are set with Y and Z-axis parallel to the floor and X normal to the floor. The crankshaft of engine is in the direction of Z-axis. Under the assumption of "small" motion, the engine-mount system equation can be written as

$$[\mathbf{M}]\{\ddot{\mathbf{x}}\} + [\mathbf{K}]\{\mathbf{x}\} = \{\mathbf{F}\}e^{i\omega t}, \tag{1}$$

where $[\mathbf{M}]$ is the 6×6 engine's rigid mass matrix, $\{\mathbf{x}^T\} = [x_g\ y_g\ z_g\ \theta_x\ \theta_y\ \theta_z]$ the displacement vector at c.g. of the engine, $[\mathbf{K}]$ the 6×6 stiffness matrix, $\{\mathbf{F}\}$ the 6×1 vector of excitation forces and moments and ω the forcing angular frequency.

The majority of mounts used in the engine mounting are of a rubber bonded to metal, or elastomeric construction. Complex spring stiffness is used to model the dynamic behavior of the mount [6]. The complex stiffness of a mount in the three directions of its local co-ordinate system is defined by the equation

$$[\mathbf{k}'] = [\mathbf{k}](1 + j\eta), \tag{2}$$

where η is the loss factor and $j = \sqrt{-1}$. The stiffness matrix must be transformed from its local-amount co-ordinate system to the global co-ordinate system situated at the engine c.g. The stiffness in the global co-ordinate system can be expressed as

$$\{\mathbf{k}_i\} = [\mathbf{A}]\{\mathbf{k}'\}[\mathbf{A}^{-1}], \tag{3}$$

where $[\mathbf{A}]$ is the transpose matrix of the Euler angle matrix [7].

The stiffness matrix $[\mathbf{K}]$ can be calculated [8] based on the stiffness matrix $[\mathbf{k}_i]$ in equation (3) and position matrix $[\mathbf{r}_i]$ of individual mount i. The displacement vector $\{\mathbf{x}\}$ in equation (1) is thus expressed as

$$\{\mathbf{x}\} = \{\mathbf{F}\}/([\mathbf{K}] - \omega^2[\mathbf{M}]). \tag{4}$$

The displacement at each mount is

$$\{\mathbf{U}\} = [\mathbf{K}_a]\{\mathbf{x}\}, \tag{5}$$

where $\{\mathbf{U}\} = \{U_{1x}, U_{1y}, U_{1z}, \ldots, U_{4x}, U_{4y}, U_{4z}\}^{\mathrm{T}}$ and

$$[\mathbf{K}_a] = \begin{bmatrix} 1 & 0 & 0 & 0 & r_{1z} & -r_{1y} \\ 0 & 1 & 0 & -r_{1z} & 0 & r_{1x} \\ 0 & 0 & 1 & r_{1y} & -r_{1x} & 0 \\ \vdots & \vdots & \vdots & \vdots & \vdots & \vdots \\ \vdots & \vdots & \vdots & \vdots & \vdots & \vdots \\ 1 & 0 & 0 & 0 & r_{4z} & -r_{4y} \\ 0 & 1 & 0 & -r_{4z} & 0 & r_{4x} \\ 0 & 0 & 1 & r_{4y} & -r_{4x} & 0 \end{bmatrix}_{(12\times 6)}. \tag{6}$$

The velocity matrix at each mounting point is

$$\{\mathbf{V}\} = \mathrm{j}\omega\{\mathbf{U}\}. \tag{7}$$

3. INVERSE EQUATIONS OF ENGINE MOTION

In the case with the known velocity at each mounting point, the displacement at c.g. of engine can be obtained from equation (5). Since there are 12 sub-equations for four mounting points but with only six variables, it is clear that there exist six sub-equations that are dependent on others. The identification of these dependent equations is difficult and the results may also vary with the change of excitation force. For solving these overdetermined matrix equations, a procedure of least-squares method is applied by changing $[\mathbf{K}_a]$ into a square matrix for inversion. $\{\mathbf{x}\}$ is thus expressed as

$$\{\mathbf{x}\} = \frac{1}{\mathrm{j}\omega}([\mathbf{K}_a]^{\mathrm{T}}[\mathbf{K}_a])^{-1}[\mathbf{K}_a]^{\mathrm{T}}\{\mathbf{V}\}, \tag{8}$$

$$\{\mathbf{F}\} = [\mathbf{Z}]\{\mathbf{V}\}, \tag{9}$$

where

$$[\mathbf{Z}] = \frac{1}{\mathrm{j}\omega}([\mathbf{K}] - \omega^2[\mathbf{M}])([\mathbf{K}_a]^{\mathrm{T}}[\mathbf{K}_a])^{-1}[\mathbf{K}_a]^{\mathrm{T}}. \tag{10}$$

$[\mathbf{Z}]$ is a 6×12 matrix and can be considered as the impedance matrix of the engine-mounting system.

Equation (9) requires the full information of velocity including amplitude and phase. However, in most of the practical situations, it is difficult to measure the absolute value of the phase of the velocity due to the phase shift caused by other factors, e.g., cable, measuring instrument, etc. But, the phase difference between V_i values can be measured especially at the same point since, normally, one transducer (accelerometer) can detect simultaneously the velocities in three directions at one point. The velocities at four mounting points are thus expressed as

$$[\mathbf{V}] = |\mathbf{V}|^{\mathrm{T}}[\mathbf{P}_v], \tag{11}$$

where $|\mathbf{V}|$ is the amplitude of the velocity which is the peak value in the velocity spectrum;

$$[\mathbf{P}_v] = [e^{jP_{1x}}\ e^{jP_{1y}}\ e^{jP_{1z}}, \ldots, e^{jP_{4x}}\ e^{jP_{4y}}\ e^{jP_{4z}}] \tag{12}$$

is the phase matrix and

$$P_{1y} = P_{1x} + C_{1y}, \qquad P_{1z} = P_{1x} + C_{1z}, \tag{13}$$

$$P_{2y} = P_{2x} + C_{2y}, \qquad P_{2z} = P_{2x} + C_{2z}, \tag{14}$$

$$P_{3y} = P_{3x} + C_{3y}, \qquad P_{3z} = P_{3x} + C_{3z}, \tag{15}$$

$$P_{4y} = P_{4x} + C_{4y}, \qquad P_{4z} = P_{4x} + C_{4z}, \tag{16}$$

In equations (13)–(16), the phase angles in the y and z directions are expressed as the sum of a constant (phase difference) with that in the x direction.

Substituting equations (11)–(16) into equation (9) and separating the real and imaginary parts, that are 12 sub-equations and are expressed as

$$\begin{bmatrix} F_x \\ F_y \\ F_z \\ M_x \\ M_y \\ M_z \end{bmatrix} = \begin{bmatrix} |z_{11}|\cos(P_{z11} + P_{1x}) & \cdots & \cdots & |z_{1-12}|\cos(P_{z1-12} + P_{4z}) \\ \vdots & \ddots & & \vdots \\ \vdots & & \ddots & \vdots \\ |z_{61}|\cos(P_{z61} + P_{4x}) & \cdots & \cdots & |z_{6-12}|\cos(P_{z6-12} + P_{4z}) \end{bmatrix} \begin{bmatrix} |V_{1x}| \\ |V_{1y}| \\ |V_{1z}| \\ \vdots \\ \vdots \\ |V_{4z}| \end{bmatrix} \tag{17}$$

and

$$\begin{bmatrix} 0 \\ 0 \\ 0 \\ 0 \\ 0 \\ 0 \end{bmatrix} = \begin{bmatrix} |z_{11}|\sin(P_{z11} + P_{1x}) & \cdots & \cdots & |z_{1-12}|\sin(P_{z1-12} + P_{4z}) \\ \vdots & \ddots & & \vdots \\ \vdots & & \ddots & \vdots \\ |z_{61}|\sin(P_{z61} + P_{4x}) & \cdots & \cdots & |z_{6-12}|\sin(P_{z6-12} + P_{4z}) \end{bmatrix} \begin{bmatrix} |V_{1x}| \\ |V_{1y}| \\ |V_{1z}| \\ \vdots \\ \vdots \\ |V_{4z}| \end{bmatrix} \tag{18}$$

Here, P_{z11} to P_{z6-12} are the phase angles of the impedance matrix $[\mathbf{Z}]$. The initial phase angle of the excitation force and moment is presumed to be zero and the phase shift of impedance and velocity is only caused by the system damping. This is the basic assumption in the direct problem. In the case that there are the phase differences between forces and moments, these differences can be defined on the left-hand side of equation (18). Since there are six force variables (F_x, F_y, F_z, M_x, M_y, M_z) and four phase variables (P_{1x}, P_{2x}, P_{3x}, P_{4x}) but with 12 equations, it indicates that this is another overdetermined matrix equation but it cannot be solved with least-square method since equations are non-linear with sine–cosine functions.

Theoretically, phase information at three points is enough to obtain a unique solution for equations (17) and (18). When the engine is only with the moment excitation which often happens at $1/2f$, $3/2f$, … [1], where f is the running frequency of engine and equals to r.p.m. value of engine divided by 60, F_x, F_y, F_z equal to zero, leaving only M_x, M_y, M_z. Phase information at two points is enough to obtain a unique solution for equations (17) and (18).

However, it is difficult to distinguish which points can be taken away and results may also vary case by case, and thus the information at all points are required.

The numerical method is applied to solve equations (17) and (18). The conventional way is to evenly select n points of P_{1x}, P_{2x}, P_{3x}, P_{4x} from $-\pi$ to π and calculate the force and moment. The solution of equations (P_{1x}, P_{2x}, P_{3x}, P_{4x}) can be obtained as the imaginary parts of force and moment equal to zero. If the step size of P_{1x}, P_{2x}, P_{3x}, P_{4x} is 0·1, the total amount of function evaluation is $64 \times 64 \times 64 \times 64 = 16\,777\,216$. The time consumption will be about 4660 h if each evaluation is 1 s. This is not feasible for application. In this paper, the optimization methods that combine genetic and gradient-based algorithms are applied to solve equations (17) and (18) and finally re-construct the force and moment of engine. This is because optimization algorithms can significantly reduce the number of combination of P_{1x}, P_{2x}, P_{3x}, P_{4x}.

4. OBJECTIVE FUNCTIONS

The optimization problem to solve equations (17) and (18) is defined as:

$$\begin{aligned} &\text{Minimize} \quad P = |P_{F_x}| + |P_{F_y}| + |P_{F_z}| + |P_{M_x}| + |P_{M_y}| + |P_{M_z}|, \\ &\text{subject to} \quad -\pi < (P_{1x}, P_{2x}, P_{3x}, P_{4x}) < \pi, \end{aligned} \tag{19}$$

where P_{F_x}, P_{F_y}, P_{F_z}, P_{M_x}, P_{M_y}, P_{M_z} are the phase angles of F_x, F_y, F_z, M_x, M_y, M_z, respectively. The input data are $|V_i|$ and C_i in equations (13)–(16). If P equals zero, P_{F_x}, P_{F_y}, P_{F_z}, P_{M_x}, P_{M_y}, P_{M_z} all will be zero. The obtained P_{1x}, P_{2x}, P_{3x}, P_{4x} values will be used to re-build [**V**] in equation (11) and the force and moment can thus be identified from equation (11) and the force and moment can thus be identified from equation (9). In the case that engine is only with moment excitation which often happens at $1/2f$, $3/2f$, $5/2f, \ldots,$ F_x, F_y, F_z will be zero. The calculated phase angles of them should also be zero. However, due to the calculation errors of real and imaginary parts, the phase angle from the numerical calculation is sometimes significantly away from zero which causes the problem in the optimization. This also happens when any force or moment equals zero. The solution to this problem is to add a small constant, e.g., 10, to the calculated force in equation (9) for the optimization. This constant will make the objective function a bit smaller but it will not change the optimization results of P_{1x}, P_{2x}, P_{3x}, P_{4x}.

5. OPTIMIZATION ALGORITHMS

There are many kinds of optimization algorithms and can be classified into two groups: one is the conventional gradient-based optimization method including quasi-Newton method, quadratic programming algorithm, etc. The other group composed of the recently developed global searching optimization methods, including genetic algorithm, simulated annealing method, etc. The gradient-based methods may not be able to find a global minimum. This is due to the fact that all the conventional gradient-based algorithms are based upon the functions with continuous first and second derivative of objective function. However, the objective function P here may not be able to satisfy this requirement since the absolute value is applied in equation (19). Another reason is that the objective function may not be able to satisfy the conditions of strict convexity [9]. Thus, the optimization results would depend on the starting points of variables. This drawback can only be overcome by selecting global searching algorithm, mainly genetic algorithm (GA) as an alternative to the classical optimization methods, which are likely to converge to a local optimum. The big advantage of this method is that it undertakes a wider search in the entire design variable space than the conventional gradient-based algorithms. This is mainly due to the random character of the procreation process in the genetic operators. This wider searching increases the probability of converging to a global minimum. Theoretically, it can always find the global minimum provided the population and generation are large enough. However, this random character of search process requires a huge amount of unproductive objective function evaluations which consume much computer time. Furthermore, unlike the gradient method which converges to only one solution for a fixed starting point, the genetic method may generate different solutions even with the same system settings. This is because the populations are randomly generated. On the other hand, the performance of GAs near the global solution appears to be relatively imprecise when compared with conventional local gradient-based techniques. Since the gradient-based algorithms and GAs cannot solve the problem for any kinds of objective functions to find a global minimum independently, a combined genetic and gradient-based method is applied and proved to be more effective in this paper. Here, the genetic method is applied to find a starting point for the gradient-based method. This is because the initial population and functional generations required to find a global minimum in GAs may be very large and is thus computational expensive. This time can be significantly reduced if it is only required to find a point near the global minimum. This point will be used as the starting point for the gradient-based method, the convergence to a global value can thus be achieved. This combination method is also applied in other inverse problem [10].

The basic genetic algorithm is as follows:

1. Create an initial population (usually a randomly generated string).
2. Evaluate all the individuals (apply some function or formula to the individuals).
3. Select a new population from the old population based on the fitness of the individual as given by the evaluation function.
4. Apply some genetic operators (mutation and crossover) to members of the population to create new solutions.
5. Evaluate these newly created individuals.
6. Repeat steps 3–5 (one generation) until the termination criteria has been satisfied (usually perform for a certain fixed number of generations).

For a detailed account of GAs, it can be referred in the text by Zalzala and Fleming [11].

The selected gradient-based method is the sequential quadratic programming (SQP) which is considered as a superior method in the conventional gradient-based algorithms for solving non-linear constrained optimization problems in terms of computer time and number of function evaluations [12]. In SQP, the objective and constraint functions are approximated using Taylor series approximations. However, a quadratic, rather than a linear approximation of objective function is used. The optimization problem is thus approximated by a quadratic programming (QP) problem at each iteration. This QP sub-program is solved using a standard QP solver. The problem terminates if the minimum is reached and all constraints are satisfied. If not, the solution of QP guarantees that the further descend is possible and approximation process repeats. An overview of SQP is found in Fletcher [13].

6. CASE STUDY

Consider a typical engine that is installed as illustrated in Figure 1. The engine is supported at four corners by four identical isolators. The location of each mount is listed in Table 1.

TABLE 1

Mounting locations of isolators

	X(m)	Y(m)	Z(m)
C.g.	0	0	0
Mount 1	− 1	0·8	2·2
Mount 2	− 1	− 1·2	2·2
Mount 3	− 1	− 1·2	− 1·8
Mount 4	− 1	0·8	− 1·8

The engine mass in 9600 kg. The mass moment of inertia $I = [I_{xx}\ I_{yy}\ I_{zz}\ I_{xy}\ I_{xz}\ I_{yz}] = [15\,100\ 15\,999\ 6399\ 2000\ 900\ 1200]\ \mathrm{kg\,m^2}$. The damping loss factor η is 0·1. The isolator stiffness are $K_x = K_y = 1{\cdot}9 \times 10^6$ N/m, $K_z = 4{\cdot}6 \times 10^7$ N/m. The running speed of engine is 1500 r.p.m. which means the running frequency of engine is 25 Hz. The orientation of each isolator is set such that, in each direction, the absolute value of angle of each mount is the same but it may be arranged in the negative direction to satisfy the balance requirement of engine installation. The arrangement of four mount orientations meet the following requirement:

$$-\alpha_1 = \alpha_2 = \alpha_3 = -\alpha_4, \tag{20}$$

$$\beta_1 = \beta_2 = -\beta_3 = -\beta_4, \tag{21}$$

$$\gamma_1 = \gamma_2 = \gamma_3 = \gamma_4, \tag{22}$$

where α, β, γ, are the Euler angles with the first rotation around positive Z-axis, then Y-axis followed by X-axis as shown in Figure 1. The selected absolute values of α, β, γ are 0, 74°, 79°, respectively.

In the direct problem, the excitation force and moment are the input parameters. The output parameter is the velocity at mounting points in three directions. For the force excitation as listed in Table 2, the velocities at mounting points are calculated based on the direct equations and listed in Tables 3 and 4.

If the real and imaginary parts in Tables 3 and 4 can be accurately measured, the excitation force and moment can be exactly re-constructed from equation (9) to obtain the force and moment in Table 2. However, the absolute values of phase are difficult to be obtained. The practical method is to pick up the velocity data with sensor at each mounting point to obtain the velocity amplitude and phase angle difference between three orthogonal directions. The input velocity amplitude for force re-construction based on the absolute values in Tables 3 and 4 is listed in Tables 5 and 6 while the input phase angles with known phase difference between three directions derived from Tables 3 and 4 are listed in Tables 7 and 8.

With the input data as shown in Tables 5–8 and the application of the genetic and SQP optimization algorithms in equations (19), P_{1x}, P_{2x}, P_{3x}, P_{4x} can be obtained. Table 9 gives the optimization results with comparison between the direct calculation of phase angles in Tables 3 and 4 and that from optimization.

It is found from Table 9 that the phase angle of velocities can be well rebuilt with the error less than 0·1% which implied that the force and moment can be exactly reconstructed. It also proves that full information on velocity is not necessary for force identification.

TABLE 2

Excitation force and moment

f (Hz)	F_x (N)	F_y (N)	F_z (N)	M_x (Nm)	M_y (Nm)	M_z (Nm)
12·5	0	0	0	10	20	80
25	4800	200	1200	65	470	230

TABLE 3

The velocity at four mounting points at 12·5 *Hz*

Velocity (mm/s)	Point 1	Point 2	Point 3	Point 4
V_x	0·0040 + 0·0705j	0·0030 − 0·0513j	0·0056 − 0·0928j	0·0014 + 0·0290j
V_y	− 0·0028 − 0·0252j	− 0·0028 − 0·0252j	− 0·0036 − 0·1869j	− 0·0032 − 0·0187j
V_z	0·0011 + 0·0194j	0·0010 + 0·0168j	0·0010 + 0·0162j	0·0011 + 0·0194j

TABLE 4

The velocity at four mounting points at 25 *Hz*

Velocity (mm/s)	Point 1	Point 2	Point 3	Point 4
V_x	0·0682 − 3·2982j	− 0·0005 − 3·6154j	− 0·0200 − 3·1000j	0·0487 − 2·7828j
V_y	− 0·1390 − 1·7388j	− 0·1390 − 1·7388j	0·2430 + 1·4835j	0·2430 + 1·4835j
V_z	0·0821 − 0·3174j	− 0·1089 − 1·9286j	− 0·1089 − 1·9286j	0·0821 − 0·3174j

TABLE 5

The velocity amplitude at four mounting points at 12·5 *Hz*

Velocity (mm/s)	Point 1	Point 2	Point 3	Point 4
$\|V_x\|$	0·0706	0·0514	0·0929	0·0291
$\|V_y\|$	0·0254	0·0254	0·0190	0·0190
$\|V_z\|$	0·0195	0·0162	0·0162	0·0195

TABLE 6

The velocity amplitude at four mounting points at 25 *Hz*

Velocity (mm/s)	Point 1	Point 2	Point 3	Point 4
$\|V_x\|$	3·2989	3·6154	3·1000	2·7832
$\|V_y\|$	1·7443	1·7443	1·5033	1·5033
$\|V_z\|$	0·3279	1·9316	1·9316	0·3279

TABLE 7

The velocity phase angles at four mounting points at 12·5 Hz

Velocity phase (rad)	Point 1	Point 2	Point 3	Point 4
P_x	P_{1x}	P_{2x}	P_{3x}	P_{4x}
P_y	$P_{1x} - 3{\cdot}3102$	$P_{2x} - 0{\cdot}1699$	$P_{3x} - 0{\cdot}2270$	$P_{4x} - 3{\cdot}3558$
P_z	$P_{1x} - 0{\cdot}0011$	$P_{2x} + 3{\cdot}1432$	$P_{3x} + 3{\cdot}1409$	$P_{4x} + 0{\cdot}0103$

TABLE 8

The velocity phase angles at four mounting points at 25 Hz

Velocity phase (rad)	Point 1	Point 2	Point 3	Point 4
P_x	P_{1x}	P_{2x}	P_{3x}	P_{4x}
P_y	$P_{1x} - 0{\cdot}1005$	$P_{2x} - 0{\cdot}0797$	$P_{3x} + 2{\cdot}9856$	$P_{4x} + 2{\cdot}9617$
P_z	$P_{1x} + 0{\cdot}2324$	$P_{2x} - 0{\cdot}0563$	$P_{3x} - 0{\cdot}0500$	$P_{4x} + 0{\cdot}2356$

TABLE 9

Comparison of phase angles between direct and inverse calculation

f		P_{1x}	P_{2x}	P_{3x}	P_{4x}
	Direct	1·6272	− 1·5131	− 1·5108	1·6180
12·5 (Hz)	Inverse	1·6272	− 1·5131	− 1·5109	1·6180
25	Direct	− 1·5501	− 1·5709	− 1·5772	− 1·5533
(Hz)	Inverse	− 1·5486	− 1·5724	− 1·5756	− 1·5551

The effectiveness of optimization methods is also investigated. It is found from Table 10 that at frequencies 12·5 and 25 Hz, the objective function values in equation (19) after genetic optimization are 0·7697 and 0·7194 respectively, with population size 1000 and generation size 500 but reduced to only 0·0003 and 0·0005 after SQP optimization. The reconstructed force and moment after GA and GA + SQP optimization are listed in Table 10 and compared with the original force and moment in Table 2. It is clear that with only GA optimization, it is difficult to achieve the requirement.

It is interesting to investigate whether the phase information requirement can be reduced from four mounting points to three points since theoretically the equation numbers from three points are enough for force re-construction. Table 11 gives the results in different groups of mounting points with the phase information. P in the table is the objective function in equation (19). It is found that, with only phase information from points 1, 2, 4 (phase difference between X, Y and Z directions), the excitation force and moment cannot be reconstructed even though the objective function is very small which means a quite successful optimization. However, the other groups in Table 11 show that the force and moment can be well re-built even with a bigger objective function value at point groups 2–4. It implies that, with less phase information, the force and moment can be rebuilt but it may also cause a significant error if this is a poorly selected group of phase information.

TABLE 10

Reconstruction of force and moment after GA and GA + SQP

f		F_x	F_y	F_z	M_x	M_y	M_z	P
12·5 (Hz)	**F** (Original)	0	0	0	10	20	80	—
	F(GA)	0·0270 + 0·1834j	− 0·689 + 1·7697j	0·593 − 2·7444j	10·353 − 2·0443j	19·737 + 3·9936j	79·848 + 6·8614j	0·7697
	F(GA + SQP)	− 0·0014 − 0·0001j	0·0020 − 0·0032j	0·001 + 0·0006j	9·993 + 0·0011j	19·999 + 0·0019j	80·00 + 0·0014j	0·7194
25 (Hz)	**F** (Original)	4800	200	1200	65	470	230	—
	F(GA)	3896·8 − 625·2j	364·6 − 7·2j	957·3 − 141·4j	40·8 + 17·8j	499·3 + 3·8j	313·6 + 16·9j	0·0003
	F(GA + SQP)	4800 − 0·1j	200·0 − 0·1j	1200· + 0·1j	65	469·9 − 0·1j	230 + 0·1j	0·0005

TABLE 11

The force and moment re-construction with the phase information at only three mounting points

Points with Phase	F_x (N)	F_y (N)	F_z (N)	M_x (Nm)	M_y (Nm)	M_z (Nm)	P (rad)
1 + 2 + 3	4799·5 + 2·7j	200·4 − 3·7j	1203·6 − 3·8j	61·7 + 10·9j	469·3 + 4·0j	229·4 + 2·2j	$3{\cdot}4\times10^{-6}$
1 + 2 + 4	2225·1	2662·4	127·2	290·9	1660·4	1007·9	$2{\cdot}52\times10^{-6}$
1 + 3 + 4	4800	200	1200	65	470	230	$1{\cdot}65\times10^{-5}$
2 + 3 + 4	4798·4 − 0·2j	199·9 − 0·1j	1198	65·2	471·1	229·6 − 0·4j	$1{\cdot}3\times10^{-3}$

7. CONCLUSIONS

This paper presents a method to identify the engine excitation forces at the c.g. of an engine from the measured velocities at the mounting points. Theoretical analysis is carried out at first to obtain the equations for the force re-construction. These indicate that with the full information of velocity (amplitude and phase) at all mounting points, the excitation force and moment at the center of gravity of engine can be exactly retrieved. To avoid the difficulty in the measurement of the absolute values of the phases, further study is carried out to investigate the possibility to re-construct the force and moment with velocity amplitude as well as the relative phase difference between three directions at each mount point. A group of overdetermined equations are derived and solved with combined genetic and SQP algorithm optimization method rather than the conventional numerical method. It is found that, with velocity amplitude and phase difference in three directions at each mounting point, the excitation force and moment can be exactly reconstructed. This method should also be applicable to other rotating machinary.

REFERENCES

1. B. PAUL 1979 *Kinematics and Dynamics of Planar Machinery*. Englewood Cliffs, NJ: Prentice-Hall, Inc.

2. J. S. TAO, G. R. LIU and K. Y. LAM *Journal of Sound and Vibration* **235**, 477–494. Design optimisation of a marine engine-mounting system.
3. GRAHAM ML GLADWELL 1996 *Applied Mechanics Review* **39**(7), S25–S34. Inverse problem in vibration—II.
4. J. VERHOEVEN 1988 *American Society of Mechanical Engineers, Journal of Vibration, Acoustics, Stress, and Reliability in Design* **110**, 307–314. Excitation force identification of rotating machines using operational rotor/stator amplitude data and analytical synthesized transfer functions.
5. C. E. SPIEKERMANN, C. J. RADCLIFFE and E. D. GOODMAN 1985 *Journal of Mechanisms, Transmissions, and Automation in Design* **107**, 271–276. Optimal design and simulation of vibration isolation system.
6. D. A. SWANSON, H. T. WU and H. ASHRAFIUON 1993 *Journal of Aircraft* **30**, 979–984. Optimisation of aircraft engine suspension systems.
7. D. T. GREENWOON 1979 *Principles of Dynamics*. Englewood Cliffs, NJ: Prentice-Hall, Inc., second edition.
8. C. M. HARRIS and C. E. CREDE 1976 *Shock and Vibration Handbook*. New York: McGRAW-HILL Inc., second edition.
9. D. M. HIMMELBLAU 1972 *Applied Nonlinear Programming*. New York: McGRAW-HILL, Inc.
10. G. R. LIU, X. HAN and K. Y. LAM (in press) *Computer Methods in Applied Mechanics and Engineering*. A combined genetic algorithm and nonlinear least square method for material characteristics using elastic waves.
11. A. M. S. ZALZAL and P. J. FLEMING 1997 *Genetic Algorithms in Engineering Systems*, IEE Control Engineering Series, Vol. 55, London: The Institute of Electrical Engineers.
12. M. POGU and J. E. SOUZA DE CURSI 1994 *Journal of Global Optimisation* **5**, 159–180. Global optimisation by random perturbation of the gradient method with a fixed parameter.
13. R. FLETCHER 1980 *Practical Methods of Optimisation*. New York: John Wiley and Sons.